Thermochimica Acta 512 (2011) 40–48

Contents lists available at ScienceDirect

Thermochimica Acta

journal homepage: www.elsevier.com/locate/tca

Vapor compression CuCl heat pump integrated with a thermochemical water splitting cycle

C. Zamfirescu, G.F. Naterer*, I. Dincer

Faculty of Engineering and Applied Science, University of Ontario Institute of Technology (UOIT), 2000 Simcoe Street North, Oshawa, ON, Canada L1H 74K

ARTICLE INFO

Article history:
Received 6 December 2009
Received in revised form 26 August 2010
Accepted 27 August 2010
Available online 9 September 2010

Keywords:
Cu–Cl thermochemical cycle
Water splitting
Hydrogen production
Heat pump
Cuprous chloride
Performance

ABSTRACT

In this paper, the feasibility of using cuprous chloride (CuCl) as a working fluid in a new high temperature heat pump with vapor compression is analyzed. The heat pump is integrated with a copper–chlorine (Cu–Cl) thermochemical water splitting cycle for internal heat recovery, temperature upgrades and hydrogen production. The minimum temperature of heat supply necessary for driving the water splitting cycle can be lowered because the heat pump increases the working fluid temperature from 755 K up to ~950 K, at a high COP of ~6.5. Based on measured data available in past literature, the authors have determined the *T–s* diagram of CuCl, which is then used for the thermodynamic modeling of the cycle. In the heat pump cycle, molten CuCl is flashed in a vacuum where the vapor quality reaches ~2.5%, and then it is boiled to produce saturated vapor. The vapor is then compressed in stages (with inter-cooling and heat recovery), and condensed in a direct contact heat exchanger to transfer heat at a higher temperature. The heat pump is then integrated with a copper–chlorine water splitting plant. The heat pump evaporator is connected thermally with the hydrogen production reactor of the water splitting plant, which performs an exothermic reaction that generates heat at 760 K. Additional source heat is obtained from heat recovery from the hot reaction products of the oxy-decomposer. The heat pump transfers heat at ~950 K to the oxy-decomposer to drive its endothermic chemical reaction. It is shown that the heat required at the heat pump source can be obtained completely from internal heat recovery within the plant. First and second law analyses and a parametric study are performed for the proposed system to study the influence of the compressor's isentropic efficiency and temperature levels on the heat pump's COP. Two new indicators are presented: one represents the heat recovery ratio (the ratio between the thermal energy obtained by internal heat recovery, and the energy needed at the heat pump evaporator), and the other is the specific heat pump work per mole of hydrogen produced. This new heat pump with CuCl as a working fluid can be attractive in other industrial contexts where high temperature heat is needed. One may replace a common heating technology (combustion or electric heating) with the present sustainable method that uses heat recovery and high efficiency temperature upgrading for heating applications.

1. Introduction

Hydrogen is recognized as an important component of the sustainable energy portfolio in the future for carbon-free society. From a sustainability perspective, hydrogen can be synthesized from water or biomass using primary energy sources which are considered sustainable (e.g., solar, wind, nuclear, hydro, geothermal, biomass, tidal, etc.). It is important to develop new commercially viable technologies which can produce hydrogen at high efficiency and reduced consumption of primary energy.

Water electrolysis is an existing commercial technology for sustainable hydrogen production. High temperature steam electrolysis – which can use a combination of sustainable thermal energy sources and electricity – represents an emerging new development for hydrogen production that promises higher efficiencies than conventional electrolysis. The main drawback of any electrolysis technique (either at low or high temperature) is the extensive need of electrical power. Regardless of the nature of the sustainable energy source, the conversion of heat to mechanical power introduces irreversibilities. Typical efficiencies of electricity production from sustainable thermal energy are as follows: concentrated solar 25% [1], geothermal plants 10–15%, ocean thermal conversion 3–5%, industrial heat recovery at typically 200 °C, 15% [2], nuclear reactors 34% [3], biomass through gasification and combined gas turbines/fuel cell systems, maximum ~40–50% (based on gasifier efficiency up to 70% [4], and gas turbine/fuel cell systems effi-

* Corresponding author. Tel.: +1 905 721 8668x2810; fax: +1 905 721 3370.
E-mail addresses: Calin.Zamfirescu@uoit.ca (C. Zamfirescu), Greg.Naterer@uoit.ca (G.F. Naterer), Ibrahim.Dincer@uoit.ca (I. Dincer).

0040-6031/$ – see front matter © 2010 Elsevier B.V. All rights reserved.
doi:10.1016/j.tca.2010.08.020

Nomenclature

COP	coefficient of performance
COP_{ex}	exergetic coefficient of performance
C_P	specific heat, kJ/mol K
f	function
h	molar specific enthalpy, kJ/mol
H	flow enthalpy, kJ
k	proportionality coefficient, Eq. (8), K^{-2}
n	number of moles, mol
P	pressure, Pa
Q	heat flux, kJ
R	universal gas constant, kJ/mol K
s	molar specific entropy, J/mol K
T	temperature, K
v	molar specific volume, m^3/mol
W	work, kJ
X	vapor quality

Greek letters

α	volumetric thermal expansion coefficient, K^{-1}
β	density thermal coefficient, Eq. (9), kg/m^3 K
η	efficiency
ρ	density, kg/m^3
χ	internal heat recovery ratio

Subscripts

0	reference value
ev	evaporator
(g)	gas
inp	input
(L)	liquid
m	melting
oxy	oxy-decomposer
P	pump
r	reaction
ref	reference
(s)	solid phase (crystal)
s	sensible heat
sat	saturation

ciency, 60–70% [5]). The irreversibilities associated with electricity generation lead to reduced overall thermal-to-hydrogen efficiency of hydrogen production through water electrolysis of about 20% (assuming 40% efficiency of electric power generation and 50% efficiency of water electrolysis).

A promising alternative to electrolysis is thermochemical cycles for water splitting. The main energy input needed by such systems is high temperature heat. Some electricity is still needed to transport materials, operate pumps, compressors, electrochemical reactions (when applied), and so forth. In all cases, the electricity usually represents a small fraction of the total energy input inventory. There are many types of thermochemical cycles currently under investigation, but the technology has not yet reached a large industrial commercialization stage.

Past literature shows that over 200 types of thermochemical water splitting cycles have been considered [6–8]. The copper–chlorine (Cu–Cl) cycle requires a heat source of 805 K. This cycle is under development by a consortium of North American institutions, co-led by Atomic Energy of Canada Limited (AECL) and the University of Ontario Institute of Technology in Canada (see [9] for a review of the recent status). The sulfur–iodine cycle has been developed in Japan, USA, France, etc. as described in [10]. A recent comparative study shows that the sulfur–iodine and copper–chlorine cycles have similar hydrogen production efficiencies; however, the first requires a much higher level of thermal energy source temperature (1123 K). The Westinghouse hybrid sulfur process and UT-3 cycle are among the most advanced in terms of their development [11]. The minimum temperature required to drive these cycles is about 1025–1175 K, for which possible sustainable energy sources are solar radiation or nuclear energy. Thus, the development of such thermochemical cycles occurs alongside the development of advanced solar concentrators and future generations of nuclear reactors that can operate at very high temperatures to either generate hydrogen or to co-generate both hydrogen and electricity [3].

Regarding the minimal temperature for driving the thermochemical cycle, a lower temperature allows a wider range of sustainable thermal energy sources. From past literature (e.g. [8]), cycles that require the lowest temperatures are as follows: Cu–Cl cycle 805 K, Li–N–I cycle 750 K and Fe–S–I cycle 725 K. The Li–N–I cycle has been proposed by the Argonne National Laboratory, US, and comprises three steps from which one is at ambient temperature. The main chemical involved in this cycle is lithium nitrate, which by thermal decomposition generates oxygen. The Fe–S–I cycle – also known as Yokohama Mark 3 – comprises also three steps with one at ambient temperature, one at 100 °C and the other at a high temperature. The main recycled chemical of this cycle is iron sulfate. The Cu–Cl, Li–N–I and Fe–S–I cycles draw special attention because they can be coupled to nuclear reactors of the current generation. For the current CANDU (CANada Deuterium Uranium) reactors, which produce nuclear heat at ~575 K, heat upgrading options must be considered in this case. Also, other thermal energy sources like industrial waste heat, biomass combustion, concentrated solar power and geothermal energy could be candidates for linkage to the aforementioned cycles, for example, by a heat pump that upgrades their temperature up to the required level. Among those three above cycles, the Cu–Cl cycle is in the most advanced stage of development, currently under development at a large lab scale demonstration [9].

Several studies have been published regarding possible solutions to upgrade the temperature of sustainable thermal energy sources, and linkage of such sources to a Cu–Cl water splitting plant. The main focus concerns the integration of a Cu–Cl plant with a CANDU nuclear reactor. In Refs. [12–14] are proposed various heat pumps that use organic (biphenyl, cyclohexane) and titanium-based working fluids to upgrade the source temperature. The mechanical energy needed to drive the heat pump is assumed to be sustainable/renewable at the origin. There are at least two major technical constraints when devising a thermo-mechanical heat pump for high temperatures: finding a suitable working fluid, and obtaining a coefficient of performance (COP) high enough to justify the use of a heat pump. If the COP is close to 1, then one would better use electric heating than a heat pump. The previous heat pumps have potential for improvement of the COP when heat recovery is applied.

Implementing internal heat recovery within the Cu–Cl cycle is essential for obtaining a high COP [3] presented a graphical description of a Cu–Cl plant with heat recovery sources. For example, the oxy-decomposer is a chemical reactor in the Cu–Cl cycle that needs heat input at the highest temperature, about 805 K. In this reactor, oxygen and molten cuprous chloride (CuCl) are produced and delivered as hot streams at a temperature close to the average reactor's temperature of 805 K. These streams must be cooled for further processing at lower temperature. There is an opportunity for heat recovery, through a heat pump that operates at a source temperature close to that of the products from which it recovers heat. Apart from the oxygen and molten cuprous chloride, the Cu–Cl plant has a high temperature exothermic reactor that can deliver heat at normally 725 K, but in principle, can be made to operate at

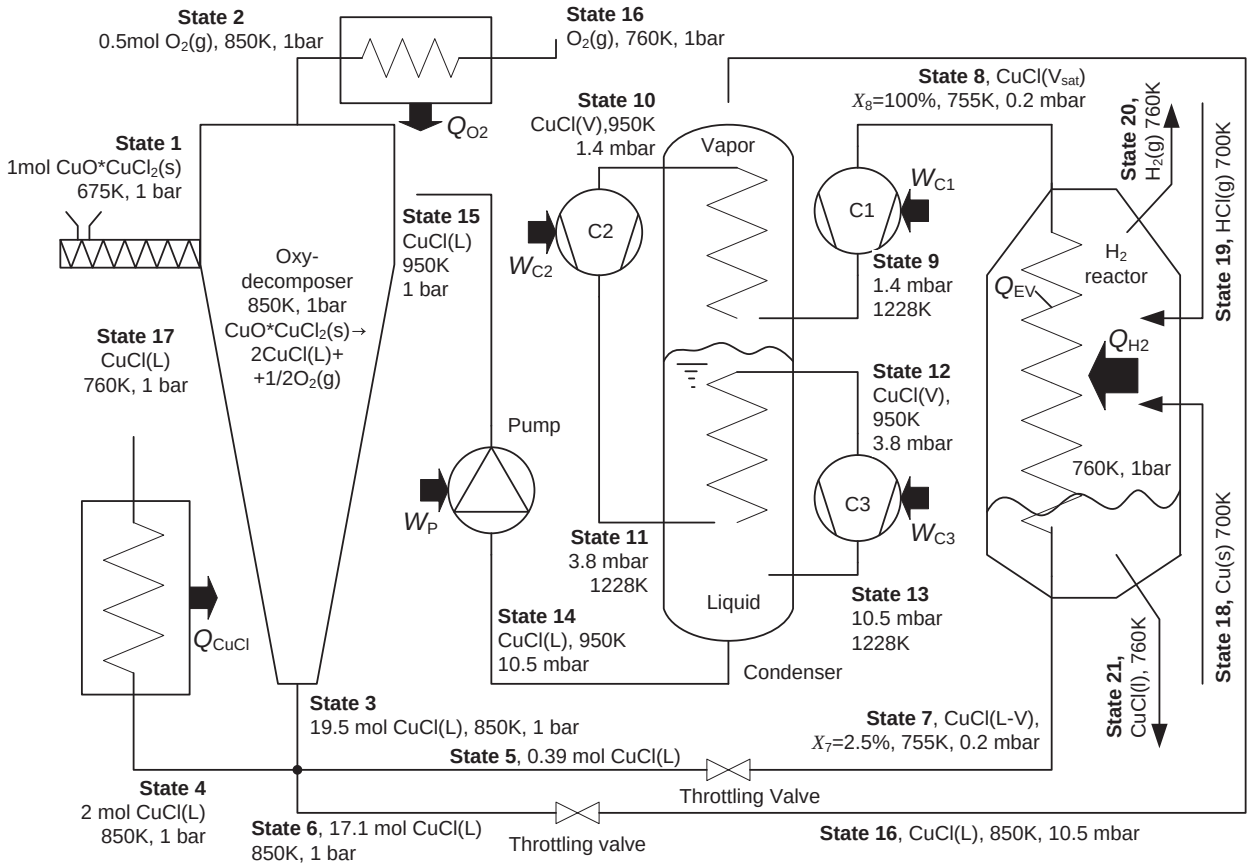

Fig. 1. Proposed heat pump system with CuCl vapor compression coupled to the oxy-decomposer (temperature and pressure values correspond to the reference case).

higher temperatures for more convenient heat recovery. Moreover, a heat pump can fill the temperature gap between a CANDU reactor (575 K) and endothermic reactors of the Cu–Cl plant (750–800 K).

In this paper, a new method of internal heat recovery for the Cu–Cl cycle is proposed at a high temperature. Heat upgrading with a reduced temperature differential assures a high COP to drive the oxy-decomposer. The heat pump is thermally coupled to the exothermic hydrogen production reactor and two hot streams of products (oxygen and molten CuCl), from which it recovers heat. The heat and temperature levels are upgraded through compressors that raise the enthalpy of cuprous chloride vapor (the working fluid). With respect to a former approach by the same authors [13], where organic and titanium based substances were studied as potential working fluids of a heat pump for internal heat recovery and temperature upgrades, in the present study one exploits the opportunity of having cuprous chlorine as the working fluid, heat transfer fluid and reaction product simultaneously. Cuprous chloride is one of the products of the oxy-decomposer, and as shown further in this paper, it may be used as the working fluid of an integrated heat pump. This allows a better thermal coupling through direct contact heat exchangers for reduced temperature gaps, which allows for higher coefficients of performance.

2. System description

This section introduces a new CuCl heat pump, which is thermally coupled with the oxy-decomposer and hydrogen production reactor of the water splitting plant. In the system shown in Fig. 1, the copper oxychloride is fed at (1) into the oxy-decomposer at 675 K. The temperatures, pressures and other parameters indicated in Fig. 1 correspond to the reference case. Inside the reactor, the particulate $CuO{\cdot}CuCl_2$ is heated by direct contact with molten cuprous chloride, which is injected at (15) at 950 K. The molten salt delivers its sensible heat and cools down to the average reactor temperature, which is assumed to be 850 K for the reference case considered in this study. The heat delivered by the hot stream in stage (15) makes copper oxychloride decompose thermally and release oxygen, while forming molten cuprous chloride (CuCl). At the top of the reactor, oxygen gas is expelled in (2), while at the bottom, molten CuCl is collected and drained out at (3). The molten CuCl product is split into three parts at the reactor exit (3): one part (4) is sent for further processing within the plant (quantitatively, state #4 flows 2 mol of CuCl for 1 mol of copper oxychloride); and the remaining two parts (streams in stages #5 and #6) are further processed thermo-mechanically within the heat pump.

The stream in stage (5) is expanded through a throttling valve in a vacuum, down to 0.2 mbar and reaches a two-phase state in (7) at a saturation temperature of 755 K. This stream is further heated and reaches 100% saturated vapor in state (8). The vapor is then compressed in three stages with intercooling in order to reduce compression work. The final pressure is 10.5 mbar, for which the corresponding saturation temperature is 950 K. A design of the condenser that embeds a direct contact heat exchanger is proposed in Fig. 1. The condenser consists of a vessel that incorporates two coils, where superheated vapors are cooled after stages 1 and 2 of compression. During the operation, at the bottom of the condenser, saturated CuCl is collected. The superheated vapor at the final stage of compression – state (13) – is injected into this liquid, and thus cooled by direct contact and condensed. The condensation heat is transferred to an additional stream of molten CuCl. This stream flows as follows (see Fig. 1):

Table 1
Equations used for steady-state modeling of the heat pump system.

Equations			Remarks
State 1: $n_1 = 1$ mol	$h_1 = \Delta_f h_{CuCl} + \Delta h_{CuCl(s)}(T_1)$		The formation enthalpy of copper oxychloride is given in Zamfirescu et al. [15] and it is $\Delta_f h_{CuCl} = -384.65$ kJ/mol; the enthalpy variation with respect to the reference temperature is given by Eq. (1).
State 2: $n_2 = 0.5$ mol	$h_2 = h(T_2, P_{ref})$		The enthalpy of oxygen at the reference pressure is taken from McBride et al. [16]. The number of moles for 1 mol of $CuO{\cdot}CuCl_2$ is denoted as n_2.
State 3: $n_3 = n_4 + n_5 + n_6$	$h_3 = h(T_3, P_{ref})$	$h_3 = h_4 = h_5 = h_6$	Streams in stages 3–6 have the same temperature, pressure, enthalpy and entropy. The enthalpy of molten CuCl is taken from McBride at al. [16] and referred to the enthalpy of the elements, which is assumed zero by convention at the reference pressure and temperature.
State 4: $n_4 = 2$ mol	$H_1 + Q_{oxy} = H_2 + H_4$		According to stoichiometry, 2 mol of CuCl are formed from 1 mol of copper oxychloride. The total enthalpy of any stream is $H_i = n_i h_i$. The energy balance on the oxy-decomposer gives the reaction heat Q_{oxy}.
State 7: $P_7 = P_{sat}(T_7)$; $h_7 = h_5 h_7 = (1 - x_7)h_{7L} + x_7 h_{7v} s_7 = (1 - x_7)s_{7L} + x_7 s_{7v}$			The saturation pressure is calculated with Eq. (7). The throttling process is isenthalpic. The mixing rule is applied to calculate the enthalpy and entropy of the state 7, which is an addition of the enthalpy of saturated liquid h_{7L} and saturated vapor h_{7v} weighted through the vapor quality x_7.
State 8: $n_8 = n_7$, $T_8 = T_7$	$h, s_8 = f(T_8)$		After complete boiling of molten CuCl, one assumes saturated vapor at the evaporator outlet and uses Eqs. (10) and (11) for entropy and enthalpy.
State 9: $n_9 = n_8$	$\eta_{C1}(h_{9s} - h_8) = h_9 - h_8$		One assumes a typical value of the isentropic efficiency of the compressor and imposes the discharge temperature $T_9 > T_{14}$.
State 10: $n_{10} = n_9$, $T_{10} = T_{14}$	$P_{10} = P_9$, $h_{10} = h(T_{10}, P_{10})$		The superheated vapor is cooled down to a temperature equal to the temperature in the condenser (see Fig. 2).
State 11: $n_{11} = n_{10}$, $T_{11} = T_9$	$\eta_{C2}(h_{11s} - h_{10}) = h_{11} - h_{10}$		One assumes that the discharge of all compression stages is at the same temperature: $T_9 = T_{11} = T_{13}$.
State 12: $n_{12} = n_{11}$, $T_{12} = T_{14}$	$P_{12} = P_{11}$, $h_{12} = h(T_{12}, P_{12})$		The superheated vapor is cooled down to a temperature equal to the temperature in the condenser (see Fig. 2).
State 13: $n_{13} = n_{12}$, $T_{13} = T_9$	$\eta_{C3}(h_{13s} - h_{12}) = h_{13} - h_{12}$		One assumes that the discharge of all compression stages is at the same temperature: $T_9 = T_{11} = T_{13}$.
State 14: $n_{14} = n_8 + n_{13}$	$P_{14} = P_{sat}(T_{14})$		Eq. (1) is used to calculate the saturation pressure of CuCl as a function of temperature. McBride et al. [16] is used to calculate the enthalpy.
State 15: $n_{15} = n_{14}$, $P_{15} = P_{ref}$	$W_p = v_{14}(P_{15} - P_{14})/\eta_P$		A typical isentropic efficiency η_P of the pump is assumed. The specific volume in state (14) is calculated through Eq. (9).
State 16: $n_{16} = n_2$, $h_{16} = h_{O_2}(T_{16})$	$H_2 = Q_{O_2} + H_{16}$		The energy balance on the heat recovery heat exchanger 2–16 gives the recovered heat flux from the oxygen, which is cooled.
State 17: $n_{17} = n_4$, $h_{17} = h_{CuCl(L)}(T_{17})$	$H_4 = Q_{CuCl} + H_{17}$		The energy balance on the heat recovery heat exchanger 4–17 gives the recovered heat flux from the molten CuCl.
State 18: $n_{18} = 2$, $T_{18} = 700$ K	$H_{18} = n_{18} h_{Cu}(T_{18})$		Particulate copper for the reaction: $2Cu(s) + 2HCl(g) \rightarrow 2CuCl(L) + H_2(g)$. The reactor operates is at 1 bar pressure.
State 19: $n_{19} = 2$, $T_{19} = T_{20}$	$H_{18} = H_{19} = H + H_{21} + Q_{H_2}$		Hot hydrochloric acid in gaseous form. Enthalpy of gaseous hydrochloric acid is evaluated at 1 bar: $H_{19} = n_{19} h_{HCl}$ (T_{19}, $P = 1$ bar).
State 20: $n_{20} = 1$, $T_{20} = 760$ K			Produced H_2 gas. Gas pressure is 1 bar. $H_{20} = n_{20} h_{H_2}$ (T_{20}, $P = 1$ bar).
State 21: $n_{21} = 2$, $T_{21} = T_{20}$			Drained cuprous chloride in molten state $H_{21} = n_{21} h_{CuCl(L)}$ (T_{21}).

- From state (6), the liquid is throttled and its pressure is reduced from 1 bar to 10.5 mbar, wherein the CuCl is still in a sub-cooled thermodynamic state; therefore, the liquid temperature does not change sensibly during the throttling (state #16);
- the subcooled liquid (16) is injected into the condenser at the top;
- inside the condenser, the enthalpy of stream in stage (16) is increased such that this stream takes all condensation heat;
- the saturated liquid collected at the bottom of the condenser (state 14 at 950 K) incorporates all condensation heat.

Furthermore, the pressure of stream in stage (14) is increased up to atmospheric pressure and then the heated flow is injected into the oxy-decomposer at state point (15). The CuCl stream is one of the products of the oxy-decomposer, and therefore injecting this substance in excess does not influence the chemical species present in the oxy-decomposer, even though it may affect the chemical equilibrium. However, because oxygen is drawn constantly out of the reactor, there is a tendency to shift the equilibrium toward the right, which compensates the tendency of shifting toward the left due to excess CuCl present in the reactor.

Fig. 1 shows the heat and mechanical power fluxes associated with various components. The heat flux Q_{O_2} rejected by the heat exchanger cools the oxygen from state (2) to state (16). The heat flux Q_{CuCl} of cooling the molten cuprous chloride from state (4) to state (17) can be recovered and used internally to provide heat to the heat pump's evaporator. A part of the evaporation heat, Q_{ev} can be supplied by these two sources. Additional sources of heat to deliver to the evaporator can be found within the water splitting plant. For example, the hydrogen production reaction, which combines particulate copper with gaseous hydrochloric acid, is exothermic and rejects heat at over 725 K. This reactor can operate also at 760 K, and the rejected heat is recovered and used to drive the heat pump. Fig. 1 suggests that the evaporator coils of the CuCl heat pump can be embedded into the hydrogen production reactor. For the proposed settings, the heat flux received by the evaporator is the summation of heat fluxes recovered from the hydrogen production reactor, and from the heat exchangers for oxygen and CuCl(L) product cooling ($Q_{EV} + Q_{H_2} + Q_{O_2} + Q_{CuCl}$).

3. Thermodynamic analysis

The chemical reaction in the oxy-decomposer has prime importance for thermochemical modeling of the system, because the operating temperature and the associated reaction enthalpy are determined from it. This is a decomposition reaction of copper oxychloride, written as $CuO{\cdot}CuCl_2(s) \rightarrow 2CuCl(L) + (1/2)O_2(g)$.

The reaction heat at 1 bar pressure from the enthalpy of products and the enthalpies of reactants are all functions of temperature. The enthalpy of copper oxychloride at state 1 is calculated with the

following equations derived by [15]. It is given by

$$\Delta h_{CuO\cdot CuCl_2(s)}(T) = 0.05372T + 0.000167T^2 - 1.74\times10^{-7}T^3 + 7.499\times10^{-11}T^4, \quad (1)$$

where the equation is valid for a reference pressure of 10^5 Pa.

Another reaction, important for the present analysis, is the hydrogen production reactor as follows: $2Cu(s)+2HCl(g)\rightarrow 2CuCl(L)+H_2(g)$. The reaction enthalpy and the temperature level are relevant data, when devising internal heat recovery and heat upgrading systems for the water splitting plant. For calculating the reaction enthalpy of both hydrogen and oxygen production reactions discussed above, the molar enthalpies of all chemicals (except copper oxychloride for which Eq. (1) is used) were based on data from [16].

This system will be modeled for steady-state operation through mass and energy balances according to first law of thermodynamics. In addition, the coefficient of performance of the heat pump system is calculated based on the second law of thermodynamics. The main equations used for modeling are compiled in Table 1. The analysis is made under the assumption of complete reactions, and the quantities are reported based on 1 mol of copper oxychloride, which is the same as 1 mol of hydrogen produced by the copper–chlorine water splitting plant.

The energy balance of the condenser is written as follows:

$$H_6 + (h_9 - h_{10})n_9 + (h_{11} - h_{12})n_{11} + H_{13} = H_{14}. \quad (2)$$

The evaporator heat flux is

$$Q_{ev} = n_7(h_8 - h_7). \quad (3)$$

Where entropy equation is not shown in Table 1, it means that the temperature and pressure in that state is specified (or it is indicated how to be calculated); the corresponding specific entropy is then calculated as function of pressure and temperature.

The total work input to operate the compressor and pumps is

$$W_{inp} = W_P + (h_9 - h_8)n_8 + (h_{11} - h_{10})n_{10} + (h_{13} - h_{12})n_{12}. \quad (4)$$

The heat pump COP according to the first law of thermodynamics is defined with

$$COP = \frac{Q_{oxy}}{W_{inp}}, \quad (5)$$

while the exergetic COP is

$$COP_{ex} = \frac{Q_{oxy}(1 - T_0/T_2)}{W_{inp}}. \quad (6)$$

The exergetic COP differs from the COP, with a Carnot factor that corresponds to the temperature of the heat sink. This temperature is the same as the temperature of the oxy-decomposer, and assumed to be the same as the temperature of the streams exiting this reactor, $T_2 = T_3 = T_4 = T_5 = T_6$. The exergetic COP represents the ratio between the "work equivalent" of the heat delivered for a useful effect, to the oxy-decomposer, and the work input provided to the compressors that drive the heat pump. The COP according to Eq. (5) represents the ratio between the heat output and work input, which is an indication of energy utilization effectiveness. Past thermodynamic data published in the literature (e.g., enthalpy and entropy measured at the reference pressure) have been used to develop the T–s diagram of cuprous chloride. In a recent paper [15], it was shown that there is a high discrepancy and lack of published data on cuprous chloride thermo-physical properties. In particular, there is a lack of data regarding the properties of the liquid phase, such as density, expansion coefficient and viscosity. As described by Zamfirescu et al. [14], there is also a discrepancy in the melting point temperature, which was reported in various studies as: 696, 703 and 709 K. Data for the melting point of 703 K was taken from [17], which is reported with an accuracy of about 1%. Therefore, a vapor compression heat pump that uses this substance as a working fluid must operate at over 703 K source temperature.

Table 2
Thermodynamic equalities used for calculating the enthalpy and entropy.

Formula	Remarks
$\left(\frac{\partial h}{\partial P}\right)_T = v(1-\alpha T)$	h, enthalpy; P, pressure; T, temperature; v, specific volume, $\alpha = \left(\frac{\partial v}{\partial T}\right)_P$ is the volumetric thermal expansion coefficient
$\left(\frac{dC_P}{\partial P}\right)_T = -T\left(\frac{\partial^2 v}{\partial T^2}\right)_P$	C_P, specific heat, defined by $C_P = \left(\frac{\partial h}{\partial T}\right)_P$
$\left(\frac{\partial s}{\partial P}\right)_T = -v\alpha$	s, entropy, defined by $\frac{C_P}{T} = \left(\frac{\partial s}{\partial T}\right)_P$

Cuprous chloride is a salt, and in general, salts form ionic liquids in the molten state. However, it appears that CuCl is an exception. According to [18], molten CuCl is an entirely molecular fluid which has determinable vapor pressure. Furthermore, vapor pressures of CuCl were measured and reported by [19] from 10 to 10^5 Pa. The vapor pressure data has been correlated by [15] based upon a Reidel-kind equation which is used in this study and given as follows:

$$P_{sat} = \exp\left(273.8096 - \frac{39240.52}{T} + 0.27747\times10^{-5}T^2 - 33.261\times\ln(T)\right), \quad (7)$$

where P_{sat} is in Pa and T is in K.

Thermodynamic data like critical pressure and temperature, normal boiling point and saturated state enthalpies are needed to calculate the T–s diagram and design the heat pump cycle which uses CuCl as working fluid. High discrepancy exists also in past reported values for the normal boiling point. Refs. [19,20] reported 1763 K with <10% accuracy, while [21,22] gave 1485 and 1482 K, respectively. Also, the critical point pressure and the predicted critical temperature were reported by [20] with 50% accuracy. In such conditions of inconsistent thermophysical data, it appears not possible to develop a highly accurate equation of state for cuprous chloride. However, for the purpose of this paper, it is sufficient to estimate the vapor and liquid enthalpies. Fortunately, satisfactory quality data was reported in the literature for the specific heat, enthalpy and entropy of liquid and gaseous CuCl for the range of temperatures of interest. The main sources were [16,21,22]. Even though these data show some differences in the solid phase prediction (especially at γ–β crystal transition), the liquid and vapor phase data appears consistent.

This paper uses the enthalpy and entropy data by [16], which also is implemented in EES (Engineering Equation Solver – Software [23]). This data was given only for the standard pressure of 1 bar and a range of temperatures. From this reference data, this paper used the thermodynamic equalities summarized in Table 2 to calculate the enthalpy and entropy for a given pressure and temperature.

The thermal expansion coefficient is known only for the solid phase for the γ-crystal, as published by [24] for T = 353–687 K:

$$\alpha(T) = \alpha_0 + k(T - 273), \quad \alpha_0 = 9.3421\times10^{-6}\,K^{-1}, \quad k = 0.072155\times10^{-6}\,K^{-2}. \quad (8)$$

This gives values between $(1.5–3)\times10^{-5}\,K^{-1}$. Also, the density of the solid phase is higher than 4000 kg/m^3, according to [19], so the specific volume is smaller than 2.5×10^{-5} m^3/mol. Thus, both the specific volume and thermal expansion coefficients may be considered nil for calculating the enthalpy and entropy variations. From Table 2, the equations indicate that the enthalpy and entropy of the solid phase do not depend on pressure. Since the working fluid in the CuCl heat pump operates close to the melting line, this line has also been represented in the T–s diagram, which is subsequently introduced.

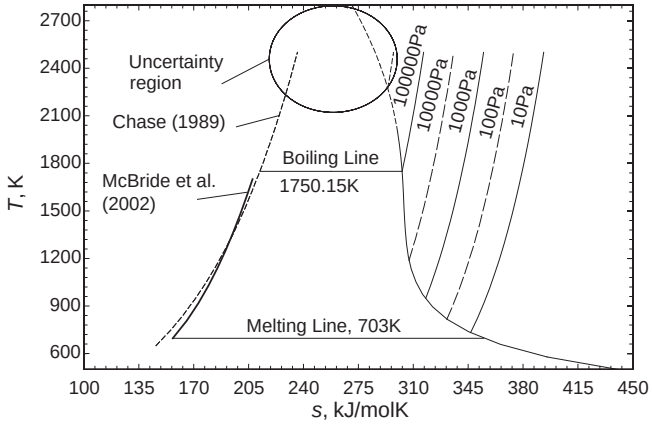

Fig. 2. *T–s* diagram of CuCl.

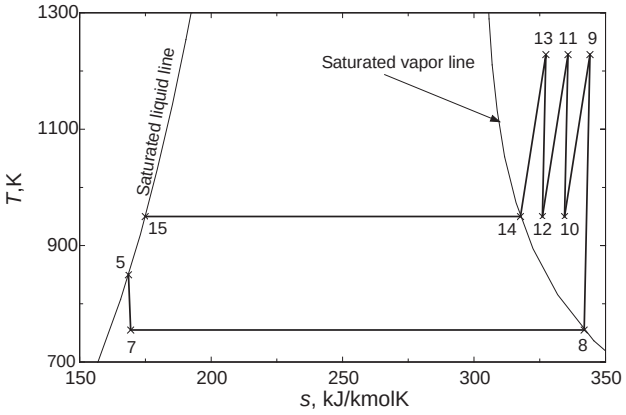

Fig. 3. Thermodynamic cycle of the CuCl heat pump.

The thermal expansion of liquid is higher than that of solid. As a first approximation, in the vicinity of the melting line, the thermal expansion coefficient is assumed to have the same order as that of the crystal, therefore it is negligible. At much higher temperatures, however, there must be a determination of the liquid's thermal expansion coefficient to calculate the enthalpy and entropy variations. However, taking in account that the range of liquid temperatures of interest is within 300 K above the melting line, the effect of thermal expansion coefficient on enthalpy and entropy variations can be neglected. From the third formula in Table 2, it appears that the entropy of liquid is insensitive to pressure. However, for calculating the enthalpy of the liquid, one must have the specific volume of the liquid. This was taken from [19], which reports the density for 703–858 K as follows:

$$\rho = \rho_m + \beta(T - T_m), \quad \rho_m = 3962\ \mathrm{kg/m^3},$$
$$\beta = 769 \times 10^{-6}\ \mathrm{kg/m^3\,K} \tag{9}$$

This shows a variation of less than 0.15 kg/m^3 for the range of temperatures of equation validity; thus the specific volume of liquid can be approximated as constant at an average value of $\bar{v}_l = 25.2 \times 10^{-6}$ m^3/mol. According to the first equation from Table 2, the liquid enthalpy variation with pressure is calculated by integrating $dh = vdp$ at constant temperature and the average value of specific volume: $h(P) = h(P_0) + \bar{v}_l(P - P_0)$, where P_0 is the standard pressure for thermodynamic tables, which is 10^5 Pa. The pressures of interest for the application vary from 10 to 10^5 Pa, at which the saturation temperature is 1750.15 K. Therefore, the expected enthalpy variation with pressure is predicted to be lower than 3 J/mol, which is a negligible quantity.

The vapor and gas phases for the range of temperatures of interest exist at low pressures, mostly at vacuum, and high temperatures, which means that the gas and vapor can be treated as ideal gases. For an ideal gas ($Pv = RT$) one has $\alpha = 1/T$ and thus $(\partial h/\partial P)_T = 0$ and $(\partial s/\partial P)_T = -P/R$. Therefore, the entropy in the vapor phase is

$$s(T, P) = s(T, P_0) + R\ \ln\left(\frac{P_0}{P}\right), \tag{10}$$

and the enthalpy

$$h(T, P) = h(T, P_0) \tag{11}$$

for all phases.

4. Results and discussion

Based on the formulae discussed above, the *T–s* diagram of CuCl has been calculated and drawn as shown in Fig. 2. The diagram has been further used to design the thermodynamic cycle of the heat pump. In order to determine the vapor pressure line, Eq. (7) has been used in a correlation to Eq. (10), where in Eq. (10), the entropy at the reference pressure has been based on data from [16]. The Riedel equation (7) has been extrapolated outside the range of pressures. However, at higher pressures, the uncertainty of vapor pressure and the vapor line become un-quantifiable. The vapor line has been computed based on data in [16]. This data has been compared on the same plot with JANAF tables of [21] – the dashed line. As described in [15], the JANAF data appears to be less accurate around the melting line. Thus, this paper used the data from [16].

Eqs. (1)–(11) and those presented in Table 1 were solved simultaneously with the solver embedded in EES software to determine the thermodynamic parameters of all state points of the cycle. Fig. 3 presents the calculated *T–s* diagram, with the state points indicated in correspondence to those from Fig. 1. A reference case has been considered in this analysis, for which the thermodynamic parameters are indicated in Figs. 1 and 3, and collected in Table 3. For the reference case, the calculated COP is 6.6, which is a value that justifies further investigations of the design and the implications of its practical realization; the assumed isentropic efficiency has been 0.85 for all compressors and the pump. Note that the isentropic efficiency represents the ratio between the power consumed for isentropic compression of the gas (or liquid pressurization in pumps) and the actual power.

Table 3
Thermodynamic parameters in all states for the reference case.

State	*T*, K	*P*, mbar	*h*, kJ/mol	*s*, J/mol K
1	675	1000	−330.3	641.6
2	850	1000	17.53	237.97
3	850	1000	−109.4	168.57
4	850	1000	−109.4	168.57
5	850	1000	−109.4	168.57
6	850	1000	−109.4	168.57
7	755	0.2	−109.4	169.11
8	755	0.2	107.8	341.85
9	1228	139.4	125.6	344.09
10	950	139.4	115.1	334.40
11	1228	382.4	126.5	335.70
12	950	382.4	115.1	326.01
13	1228	1049	125.6	327.32
14	950	1049	−103.6	174.93
15	950	1000	−103.6	174.93
16	760	1000	14.49	234.19
17	760	1000	−114.7	161.99
18	700	1000	10.4	55.09
19	700	1000	−80.49	211.93
20	760	1000	13.52	158.02
21	760	1000	−114.7	161.99

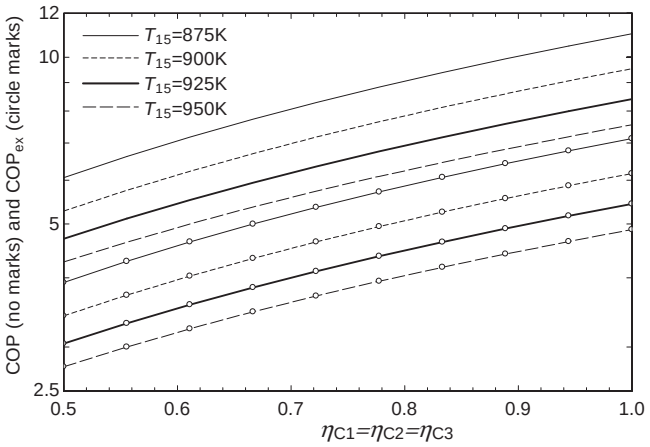

Fig. 4. Compressor isentropic efficiency and various sink temperatures.

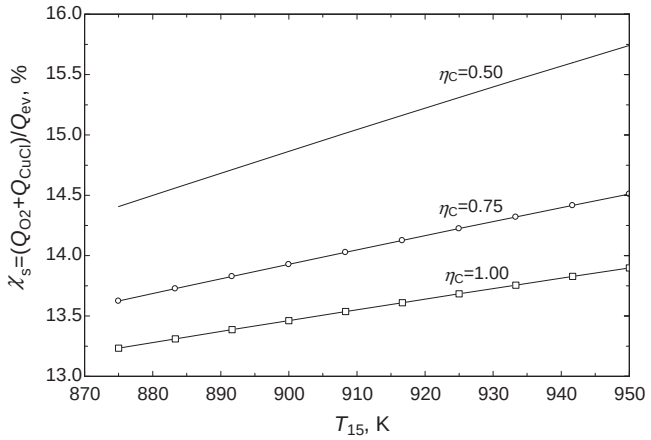

Fig. 6. Internal heat recovery ratio (χ, Eq. (11)) vs. sink temperature.

In Fig. 4, one shows the influence of the compressor's isentropic efficiency on the heat pump COP (both, energetic and exergetic). For calculating these results, the same isentropic efficiency has been assumed for all three compressors. A large range of isentropic efficiencies has been considered, from 0.5 to 1. The isentropic efficiency influences the thermodynamic parameters at the compressor's discharge and the overall efficiency of the heat pump. The upper bound of this range cannot be reached in real applications; however, we extended the calculation up to the unit compressor isentropic efficiency in order to observe the theoretical maximum COP achievable by the system. One can observe that the COP is reasonably high. This is a consequence of the rarefied state of the compressed vapor, which is at sub-atmospheric pressure. The COP is influenced by the temperature at state 15, which is the same as the temperature at which the heat pump delivers useful heat to the oxy-decomposer. If this temperature is higher, the compressors must consume more power for generating the same amount of heat at the sink. This decreases the overall system efficiency.

The additional flow rates of molten cuprous chloride that must be circulated through the reactor, for stream in stage (5) – where the CuCl has the role of the working fluid within the heat pump, and that of stream in stage (6) – where the CuCl has the role of heat carrier, depending on the temperature at which the hot stream of molten CuCl is injected into the oxy-decomposer. For a higher temperature, the flow rate is lower at 15. Fig. 5 shows the calculated values of these flow rates, with respect to the stream of product, which is molten CuCl delivered for further processing in (4). Thus,

Fig. 5 presents the ratios n_3/n_4, n_5/n_4, and n_6/n_4. It can be observed that the total flow rate of molten CuCl that leaves the reactor (n_3) is more than ~10 times higher than the stoichiometric amount (n_4) of CuCl. On the other hand, the amount of molten salt that is used as a working fluid in the heat pump (n_6) represents only ~20% of the stoichiometric flow rate.

As discussed above, a part of the heat needed by the heat pump evaporator is supplied "internally" by heat recovery from the oxygen (2–16) and molten salt (4–17) heat exchangers. It is important to know in percentages how much is the heat supplied to the heat pump through heat recovery. The following heat recovery indicator, called an internal heat recovery ratio from sensible heat, is defined as

$$\chi_s = \left(\frac{Q_{O_2} + Q_{CuCl}}{Q_{ev}} \right). \tag{12}$$

The internal heat recovery ratio from sensible heat is shown in Fig. 6 as a function of the hot fluid temperature T_{15}, and three values of the isentropic efficiency, assumed to be the same for all compressors. It shows that about 15% of the required heat to drive the heat pump evaporator is obtained by internal heat recovery within the system, from the CuCl(l) and O_2(g) cooling heat exchangers. If more heat is recovered, then a higher temperature T_{15} could be obtained.

It is also possible to perform the oxygen production reaction at a higher temperature. If the temperature of the reactor increases, more heat can be recovered from the output streams. In Fig. 7, the internal heat recovery ratio is calculated for a practical range of

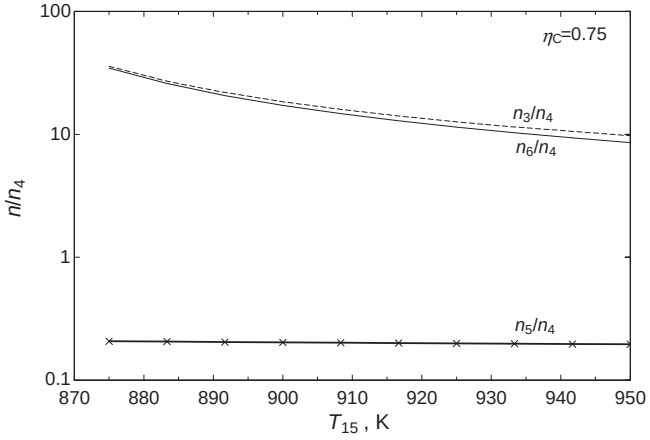

Fig. 5. Additional streams of molten CuCl given with respect to the product molar flow n_4.

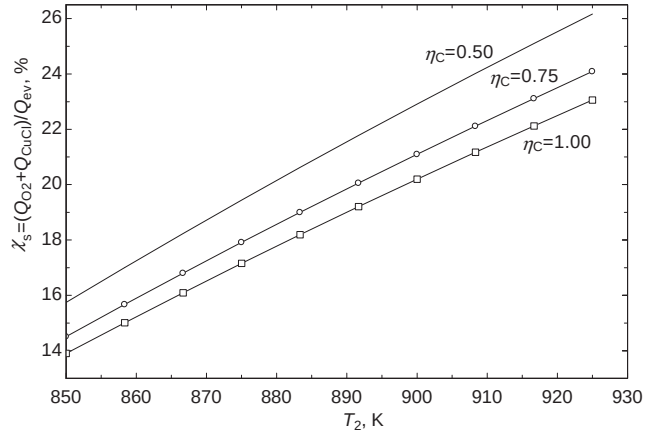

Fig. 7. Internal heat recovery ratio (χ, Eq. (11)) vs. reaction temperature, $T_2 = T_3$.

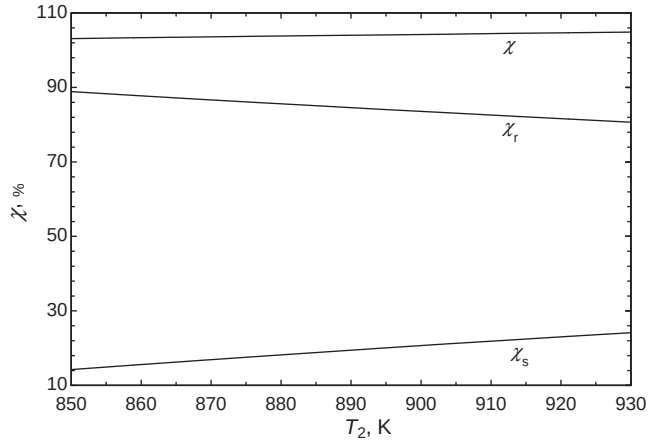

Fig. 8. The heat recovery ratio for a range of reaction temperature and $\eta_{C1,1,2} = 0.75$.

reaction temperature. It is observed that the internal heat recovery ratio can reach values of over 25%.

The remaining part of heat (~75%) must be provided from additional sources. The main sources of heat may be the heat rejected by the hydrogen production reactor of the copper chlorine water splitting plant, in which, as mentioned above and shown in Fig. 1, the heat pump evaporator coil can be placed. The heat recovery ratio from the reaction heat is defined as follows

$$\chi_r = \frac{Q_{H_2}}{Q_{ev}}, \tag{13}$$

where Q_{H_2} is the heat generated by the hydrogen production reaction (assuming that the reactor is perfectly insulated and all heat is transferred to the CuCl working fluid). Additionally, one defines the total heat recovery ratio by adding Eqs. (12) and (13): $\chi = \chi_s + \chi_r$. With these indicators, the plot from Fig. 8 has been constructed for a fixed isentropic efficiency of all compressors as 0.75.

The heat generated by the hydrogen production reactor represents over 80% of the heat needed by the CuCl heat pump evaporator. When the hydrogen reaction heat and sensible heat from hot oxygen and molten cuprous chloride salt are all recovered, the total heat recovery ratio has values of over 103%. Thus, one may conclude that all of the heat needed by the evaporator can be provided through internal heat recovery at high temperature within the water splitting plant.

The final result indicates – in Fig. 9 – the work needed to drive the heat pump system associated with production of 1 mol of hydrogen.

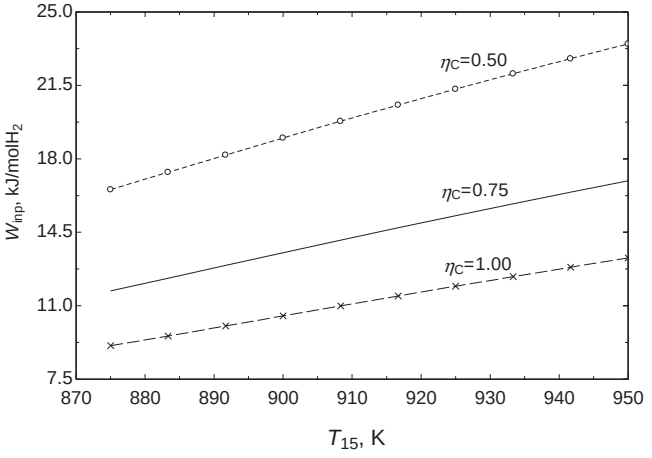

Fig. 9. Specific molar work to drive the heat pump.

This work is calculated according to Eq. (4) for a fixed temperature in the oxy-decomposer ($T_2 = 850$ K) and a range of temperatures at the heat pump sink, T_{15}. Three values were considered for the compressor's isentropic efficiency, which is taken to be the same for all compressors. The plot shows that for a reasonable isentropic efficiency of 0.75, the specific work needed to drive the pump is around 15 kJ/mol of produced hydrogen. Moreover, one observes that further increases in isentropic efficiency lead to an important reduction of the specific work.

5. Conclusions

In this paper, a novel heat upgrading system, applicable to the copper–chlorine thermochemical water splitting cycle, was proposed. The system is designed to drive the oxy-decomposer, which is the reactor operating at the highest temperature within the cycle. For a higher reaction temperature in the oxy-decomposer, the amount of heat needed to drive the chemical reaction is lower. For the molten CuCl, the vapour pressure had been measured and reported in past literature, so the *T–s* diagram was constructed for this substance and the possibility of using it is as a working fluid in a heat pump was investigated.

This study has demonstrated that CuCl can be used as working fluid in a vapour compression heat pump and that the oxy-decomposer of the Cu–Cl thermochemical plant can be linked with a CuCl heat pump system. Since the CuCl is the same chemical as the one produced at the output of the oxy-decomposer (which operates as a once-though reactor and no separation is required since the decomposition is thermal), the use of direct heat exchange is possible. Larger flow rates of CuCl than the stochiometric product can be circulated through the oxy-decomposer. The additional CuCl stream enters at higher temperature and delivers sensible heat to the reaction. The additional amount is retrieved at the reactor exit and used further in two ways: as a working fluid in the heat pump and as a heat transfer fluid. The results show that the additional – recycled – CuCl streams are more than 10 times the amount produced by the reactor.

Direct contact heat exchange has been also used in the condenser of the heat pump, which operates in a vacuum at ~10 mbar. In the condenser, molten CuCl is heated up to a high temperature, while in the chemical reactor. The COP of the heat pump is high, above 4 and typically around 6.5. Therefore, the heat pump is attractive and deserves further attention. The high COP is explained by the relatively low specific work consumed by the compressors (which operate in a vacuum and with inter-cooling), and also through internal heat recovery.

Another aspect relates to the possibility of internal heat recovery (within the heat pump). In this respect, the heat from the hot stream of products (oxygen gas and molten cuprous chloride) can be recovered and used to drive the heat pump evaporator. Up to 25% from the source heat of the heat pump can be provided from streams that are cooled. In addition, a significant amount of heat can be recovered from the exothermic hydrogen production reactor of the plant. From the results in this paper, it is possible to drive the evaporator of the heat pump in proportion of 100% with heat recovered internally from the hydrogen production reactor, and from the oxygen and molten salt heat exchangers.

This study has shown that coupling the Cu–Cl plant with a CuCl heat pump is possible and beneficial. However, the actual implementation of the solution has further technical challenges to be overcome. There is sufficient technological knowledge regarding the design of turbomachines operating at high temperature, and older designs can be adapted to operate with corrosive working fluids. There is still a lack of thermodynamic properties of the molten and gaseous CuCl, so further research is needed on the pro-

prieties such as viscosity, thermal conductivity, specific volume, critical point and others needed for design, parametric studies and simulations. It will also be useful to further study the impact of the heat pump system on the operational efficiency of the overall water splitting cycle. Other possible applications of the CuCl high temperature heat pump can also be investigated.

Acknowledgements

The authors acknowledge the support provided by the Natural Sciences and Engineering Research Council of Canada in Canada, the Ontario Research Fund and Atomic Energy of Canada Limited.

References

[1] C. Zamfirescu, I. Dincer, W.R. Wagar, Evaluation of exergy and energy efficiencies of photo-thermal solar radiation conversion, Applied Solar Energy 45 (2009) 213–223.
[2] C. Zamfirescu, I. Dincer, Thermodynamic analysis of a novel ammonia-water trilateral Rankine cycle, Thermochimica Acta 477 (2008) 7–15.
[3] C. Zamfirescu, I. Dincer, G.F. Naterer, Upgrading of waste heat for combined power and hydrogen production with nuclear reactors, Journal of Engineering for Gas Turbines and Power 132 (102911) (2010) 1–9.
[4] Y. Kalinci, A. Hepbasli, I. Dincer, Biomass-based hydrogen production: a review analysis, International Journal of Hydrogen Energy 34 (2009) 8799–8817.
[5] I. Dincer, M.A. Rosen, C. Zamfirescu, Exergetic performance analysis of a gas turbine cycle integrated with solid oxide fuel cells, Journal of Energy Resources Technology 131 (032001) (2009) 1–11.
[6] B.W. McQuillan, L.C. Brown, G.E. Besenbruch, R. Tolman, T. Cramer, B.E. Russ, B.A. Vermillion, B. Earl, H.T. Hsieh, Y. Chen, K. Kwan, R. Diver, N. Siegal, A. Weimer, C. Perkins, A. Lewandowski, High efficiency generation of hydrogen fuels using solar thermochemical splitting of water, in: Annual Report, GA-A24972, General Atomics, San Diego, 2002.
[7] M. Lewis, A. Taylor, High temperature thermochemical processes, DOE hydrogen program, in: Annual Progress Report, Washington, 2006, pp. 182–185.
[8] S. Abanades, P. Charvin, G. Flamant, P. Neveu, Screening of water-splitting thermochemical cycles potentially attractive for hydrogen production by concentrated solar energy, Energy 31 (2006) 2805–2822.
[9] G.F. Naterer, S. Suppiah, M. Lewis, K. Gabriel, I. Dincer, M.A. Rosen, M. Fowler, G. Rizvi, E.B. Easton, B.M. Ikeda, M.H. Kaye, L. Lu, I. Pioro, P. Spekkens, P. Tremaine, J. Mostaghimi, J. Avsec, J. Jiang, Recent Canadian advances in nuclear-based hydrogen production and the thermochemical Cu–Cl cycle, International Journal of Hydrogen Energy 34 (2009) 2901–2917.
[10] K. Onuki, Y. Inagaki, R. Hino, Y. Tachibana, Research and development on nuclear hydrogen production using HTGR at JAERI, Progress in Nuclear Energy 47 (2005) 496–503.
[11] C. Forsberg, Futures for hydrogen produced using nuclear energy, Progress in Nuclear Energy 47 (2005) 484–495.
[12] C. Zamfirescu, G.F. Naterer, I. Dincer, Upgrading of waste heat for combined power and hydrogen production with nuclear reactors, Journal of Engineering for Gas Turbines and Power 132 (102911) (2009) 1–9.
[13] C. Zamfirescu, I. Dincer, G.F. Naterer, Performance evaluation of organic and titanium based working fluids for high temperature heat pumps, Thermochimica Acta 496 (2009) 18–25.
[14] C. Zamfirescu, G.F. Naterer, I. Dincer, Reducing greenhouse gas emissions by a copper–chlorine water splitting cycle driven by sustainable energy sources for hydrogen production, in: Global Conference on Global Warming, Istanbul, 5–9 July, 2009, Paper #537.
[15] C. Zamfirescu, I. Dincer, G.F. Naterer, Thermophysical properties of copper compounds in copper–chlorine thermochemical water splitting cycles, International Journal of Hydrogen Energy 35 (2009) 4839–4852.
[16] B.J. McBride, M.J. Zehe, S. Gordon, NASA Glenn coefficients for calculating thermodynamic properties of individual species, in: NASA/TP—2002-211556, Washington, 2002.
[17] R.H. Perry, D.W. Green, J.O. Maloney, Perry's Chemical Engineers Handbook, 7th ed., McGraw-Hill Inc., New York, 1997.
[18] J.G. Powels, Is molten cuprous chloride a molecular liquid? Journal of Physics C: Solid State Physics 8 (1975) 895–906.
[19] D.R. Lide, CRC Handbook of Chemistry and Physics, CRC Press, Boca Raton, 2005.
[20] R.L. Rowley, W.V. Wilding, J.L. Oscarson, Y. Yang, N.F. Giles, DIPPR® Data Compilation of Pure Chemical Properties, AIChE, Taylor and Francis, New York, 2010.
[21] M.W. Chase Jr., NIST-JANAF themochemical tables, Journal of Physical and Chemical Reference Data, 4th ed., Monograph 9 (1989) 1–1951.
[22] O. Knacke, O. Kubaschewski, K. Hesselmann, Thermochemical Properties of Inorganic Substances, Springer, Berlin, 1991.
[23] S.A. Klein, Engineering Equation Solver v.8.400 F-Chart Software, 2009.
[24] K. Nitsch, M. Rodová, Thermomechanical measurements of lead halide single crystals, Physica Status Solidi B 234 (2002) 701–709.